Published in final edited form as:
Am J Physiol Cell Physiol. 2007 March ; 292(3): C1156–C1166. doi:10.1152/ajpcell.00397.2006.

Ca^{2+} sparks and T tubule reorganization in dedifferentiating adult mouse skeletal muscle fibers

Lisa D. Brown[1], **George G. Rodney**[2], **Erick Hernández-Ochoa**[3], **Chris W. Ward**[3,4], and **Martin F. Schneider**[3]

[1] *Biology Department, Morgan State University, Baltimore, Maryland* [2] *Medical Biotechnology Center, University of Maryland Biotechnology Institute, Baltimore, Maryland* [3] *Department of Biochemistry and Molecular Biology, School of Medicine, Baltimore, Maryland* [4] *School of Nursing, University of Maryland Baltimore, Baltimore, Maryland*

Abstract

Ca^{+} sparks are rare in healthy adult mammalian skeletal muscle but may appear when adult fiber integrity is compromised, and occur in embryonic muscle but decline as the animal develops. Here we used cultured adult mouse flexor digitorum brevis muscle fibers to monitor occurrence of Ca^{2+} sparks during maintenance of adult fiber morphology and during eventual fiber morphological dedifferentiation after various times in culture. Fibers cultured for up to 3 days retain normal morphology and striated appearance. Ca^{2+} sparks were rare in these fibers. At 5–7 days in culture, many of the original muscle fibers exhibit sprouting and loss of striations, as well as the occurrence of spontaneous Ca^{2+} sparks. The average rate of occurrence of Ca^{2+} sparks is >10-fold higher after 5–7 days in culture than in *days 1–3*. With the use of fibers cultured for 7 days, application of the Ca^{2+} channel blockers Co^{2+} or nifedipine almost completely suppressed the occurrence of Ca^{2+} sparks, as previously shown in embryonic fibers, suggesting that Ca^{2+} sparks may be generated by similar mechanisms in dedifferentiating cultured adult fibers and in embryonic fibers before final differentiation. The sarcomeric disruption observed under transmitted light microscopy in dedifferentiating fibers was accompanied by morphological changes in the transverse (T) tubular system, as observed by fluorescence confocal imaging of both an extracellular marker dye and membrane staining dyes. Changes in T tubule morphology coincided with the appearance of Ca^{2+} sparks, suggesting that Ca^{2+} sparks may either be a signal for, or the result of, disruption of DHPR-ryanodine receptor 1 coupling.

Keywords

calcium ion signaling; muscle remodeling; fluo 4; calcium ion imaging

Ca^{2+} sparks are brief localized elevations of cytosolic Ca^{2+} generated by the opening of a small number of ryanodine receptor (RyR) Ca^{2+} release channels (4). In frog skeletal muscle fibers, the global Ca^{2+} transient during fiber depolarization appears to be made up of the near-synchronous occurrence of large numbers of Ca^{2+} sparks throughout the muscle fiber (15). Although spontaneous Ca^{2+} sparks can be easily evoked under physiological conditions in resting adult frog skeletal muscle fibers, Ca^{2+} sparks are not normally detected in adult mammalian skeletal muscle. In fact, in adult mammalian myofibers, spontaneous Ca^{2+} sparks

Address for reprint requests and other correspondence: M. F. Schneider, Dept. of Biochemistry and Molecular Biology, Univ. of Maryland Baltimore School of Medicine, 108 N. Greene St., Baltimore, MD 21201 (e-mail: mschneid @umaryland.edu).

seem to appear only when the integrity of the fiber is compromised (i.e., permeabilized or membrane disrupted; see Refs. 7,13, and 22) or the myofiber is under acute mechanical/ionic stress (26), leading to the conclusion that Ca^{2+} spark activity is suppressed rather than nonexistent in adult mammalian myofibers (19).

In contrast to adult myofibers, Ca^{2+} sparks are normally present in embryonic mammalian skeletal muscle (7) and during early postnatal maturation of mammalian skeletal muscle (6). However, the frequency of event occurrence decreases postnatally (6) as the animal and the muscle fiber transverse (T) tubules (11) develop. Early hypotheses to explain the postnatal decline in Ca^{2+} sparks in mammalian skeletal muscle focused on differential expression of RyR isoforms (RyR1 and RyR3) during development; however, these hypotheses were quickly discounted as RyR1, as well as RyR3, was capable of producing Ca^{2+} spark-type release (7, 27). More recently, work has focused on developmental structural differences in DHPR-RyR1 coupling (1,10,21,22,31), as well as acute structural alterations at the level of the T tubules (26), showing that both are associated with Ca^{2+} sparks in adult mammalian muscle. We therefore hypothesized that experimentally induced alterations in T tubule morphology may be needed to allow spontaneous Ca^{2+} release events to occur.

We have previously utilized enzymatically dissociated adult mouse flexor digitorum brevis (FDB) muscle fibers to characterize the process of dedifferentiation of adult skeletal muscle fibers in culture. Fibers cultured for up to 3 days in serum-containing medium retain normal morphology and striated appearance. At 5–7 days in culture, many fibers begin to exhibit a change in the adult morphology, characterized by sprouting, fusion with mononuclear cells (presumably myoblasts), and loss of striations, generally beginning at their ends (2). Whether or not the morphological loss of striations and drastic changes in fiber shape observed in cultured fibers represent only fiber remodeling to the developmentally preceding terminal myotube stage, or whether this is true dedifferentiation to a precursor cell type (8,18), remains to be determined. Similar morphological regression and/or reversion to a precursor cell type occurs in vivo in muscle diseases (3) and presumably also accompanies in vivo muscle regeneration after muscle damage. Possible reversion of muscle fibers to precursor cell types (17,25) has important implications for remodeling of muscle and for “engineered” muscle or other tissues. In addition to the pronounced morphological changes observed during fiber dedifferentiation in culture, functional changes were also evident. Multiple or delayed Ca^{2+} transients in response to brief field stimulation were often observed in dedifferentiated fibers (2), indicating alterations in action potential initiation and possibly in excitation contraction (EC) coupling.

Here we use dissociated adult mouse FDB muscle fibers to monitor the occurrence of Ca^{2+} sparks during periods of maintained adult fiber morphology, and during eventual fiber morphological dedifferentiation after various times in culture. We find that Ca^{2+} sparks are extremely rare in acutely dissociated adult mouse FDB fibers or in fibers maintained for up to 3 days in culture in serum-containing medium. At 5–7 days in culture, the frequency of Ca^{2+} sparks increases, coincident with the changes in morphology indicative of dedifferentiation. As in embryonic fibers (6), Ca^{2+} channel blockers almost completely suppress the occurrence of Ca^{2+} sparks in adult fibers cultured for longer than 7 days. These observations suggest that Ca^{2+} sparks may be generated by similar mechanisms in dedifferentiating cultured adult fibers and in embryonic fibers before final differentiation. Also, changes in T tubule morphology in dedifferentiated fibers coincided with the appearance of Ca^{2+} sparks, suggesting that Ca^{2+} sparks may either be a signal for, or the result of, disruption of DHPR-RyR1 coupling.

MATERIALS AND METHODS

Preparation of isolated adult mouse skeletal muscle fibers

Single muscle fibers from the FDB muscle were enzymatically dissociated and cultured using a modified protocol previously described (16). Briefly, FDB muscles were incubated in minimal essential media containing 10% FBS and 0.2% Type I collagenase at 37°C for 2.5 h. To release single fibers, the FDB muscles were then triturated gently in media without collagenase. The fibers were then plated on laminin-coated cover slip floors of culture dishes in serum-containing media and incubated in 5% CO_2 at 37°C until use. For cultures maintained in serum-free media, the serum-containing media was replaced after 1 h of plating with minimal essential media containing 5 μg/ml apotransferrin, 5 ng/ml sodium selenite, and 5 μg/ml insulin. All images and data presented here were obtained from living cultured fibers bathed in Ringer solution (in mM: 145 NaCl, 4 KCl, 1.8 $CaCl_2$, 1 $MgSO_4$, 10 glucose, and 10 HEPES-Na_2, pH 7.4) with or without additions, as indicated, and studied at room temperature.

Imaging local Ca^{2+} sparks

Cultures of FDB fibers were loaded by exposure to 20 μM fluo 4-AM (Ca^{2+} indicator dye; Invitrogen, Carlsbad, CA) prepared in Ringer solution for ~45–60 min followed by a rest period of 15 min to allow for dye deesterification. Both fibers that appeared normal and dedifferentiating fibers were imaged for spontaneous Ca^{2+} sparks on an inverted microscope [Olympus IX-71 with a ×60, 1.3 numerical aperture (NA) water-immersion objective] coupled to a Bio-Rad CellMap IC laser scanning confocal imaging system (LSCM). Fibers that appeared normal were characterized by a striated appearance, rounded ends, and no sprouts and exhibited no visible signs of damage. Dedifferentiating fibers were characterized by loss of striations and sprouting either at the ends or from the middle of the fiber. In the basal condition, a sequence of 50 *x-y* images (512 × 512 pixels; 0.18 μm pixel; 2 ms/line) were collected at 3-s intervals shortly after deesterification of the fluo 4-AM. In each myofiber, an image sequence was taken at each end and near the midpoint of the myofiber. In a subset of the myofibers, imaging was repeated following application of Ringer solution containing Ca^{2+} channel blockers (5 μM nifedipine or 5 mM $CoCl_2$). Image sequences were processed, and the frequency of sparks was determined as described in Chun et al. (6). In brief, Ca^{2+} sparks were identified using a modified automatic detection method as previously described (5,6). In this method, the mean fiber fluorescence image was determined by a pixel-by-pixel average of a 25-image sequence. In each sequence, potential local Ca^{2+} release events were identified as contiguous pixels exhibiting fluorescence ≥1.5 SDs above the mean fiber fluorescence. Regions selected as local Ca^{2+} events were identified in ΔF/F (where F is fluorescence) images as contiguous regions of pixels having fluorescence values greater than or equal to two SD above the mean fluorescence for the same pixel, and were selected by the criterion that at least one pixel within the two SD area must exceed three SD above the mean.

Line scan images

The temporal profiles of the Ca^{2+} spark were assessed with linescan (*x-t*; distance-time) images (5-s acquisition time, 2 ms/line, 512 pixels/line, 0.18 μm/pixel) of fluorescence of fluo 4-loaded fibers. Regions of interest (ROI) in which potential Ca^{2+} sparks occurred were detected by an automatic computer detection algorithm (20) as modified from Cheng et al. (5). Images were corrected for PMT offset and then converted to ΔF by subtraction of the spatial (*x*) pattern of resting fluorescence (F) along the fiber averaged in time over the entire duration, excluding the contribution of potential Ca^{2+} spark ROIs. ΔF images were then normalized pixel-by-pixel by F and smoothed 3 × 3 to create ΔF/F normalized images.

Fiber resting Ca^{2+} concentration measurements

Intracellular free Ca^{2+} measurements were carried out with a ratiometric fluorescence method using the Ca^{2+} fluorescent probe indo 1. Fibers were rinsed with Ringer solution and loaded with indo 1-AM (4 μM; Invitrogen) for 45 min at room temperature. After being loaded, fibers were washed with dye-free Ringer solution followed by a rest time interval of 20 min to allow deesterification of the probe. Intracellular free Ca^{2+} measurements were performed at room temperature. A photometry system, data acquisition board PCI-6221, and custom-made software written in LabView (National Instruments, Austin, TX) were used to acquire and analyze fluorescence data. Fibers were illuminated with a xenon-arc lamp (300 W, Lambda LS; Sutter Instruments, Novato, CA) only during recording of light signals to minimize photobleaching. The ratiometric method and the calibration procedure have been published elsewhere (12). The ratio (R) of the dual emission fluorescence of the free and Ca^{2+}-bound forms of indo 1 (at 485 and 405 nm, respectively) were separated, filtered, and collected by two photomultipliers. The light signals were collected from a spot of ~15 μm diameter. This procedure allowed the recording at various locations in the same fibers and reduced ultraviolet light exposition. Intracellular calibration experiments were performed to convert ratios to Ca^{2+} concentration ($[Ca^{2+}]$). R_{min} was determined by exposing the muscle fibers to a zero Ca^{2+} Ringer solution with 20 μM 4-bromo A-23187, a nonfluorescent Ca^{2+} ionophore (Invitrogen), pH 7.4. When the fluorescence reached a steady minimum value (R_{min}), fibers were exposed to a high-Ca^{2+} (20 mM) Ringer solution and 20 μM 4-bromo A-23187 to estimate R_{max}. The following equation published by Grynkiewicz et al. (12) and modified to correct for dye compartmentalization by Zhou et al. (31) was used to convert ratios to $[Ca^{2+}]$

$$[Ca^{2+}]=K_{eff}[(R - R_0)/(R_{max} - R)]b$$

where b is the ratio of the 485-nm signals at zero and saturating $[Ca^{2+}]$. K_{eff} and R_0 are effective values of the dissociation constant and R_{min}, respectively. We assumed a constant and similar contribution of volume of sarcoplasmic reticulum (SR) and mitochondria in adult and dedifferentiated muscle fibers (<10% of total) as that reported by Zhou et al. (31) in myotubes. K_{eff} was calculated to be 400 nM. When translating ratios into $[Ca^{2+}]$, the K_{eff} acts as a constant scaling factor; hence, any possible underestimation in K_{eff} will not markedly affect the differences observed in the results.

Block of plasma membrane and T tubule Ca^{2+} channels

Ca^{2+} channel blockers were applied either by draining the chamber and adding blockers at the final desired concentration in Ringer solution or by removing 1 ml of the 2-ml solution in the chamber and adding 1 ml of 2× concentration of inhibitor in Ringer solution.

Visualization of T tubular system in living fibers

T tubules of FDB fibers were visualized by using three alternative procedures, as follows: *1*) sulforhodamine B staining: Cultured myofibers were exposed to the fluorescent dye sulforhodamine B (100 μM; Polysciences, Rydal, PA) in Ringer solution. After a brief incubation, this extracellular marker dye diffuses into the T tubular system (9) and allows visualization of the T tubule morphology by confocal fluorescence microscopy (excitation: 550 nm; emission: >585 nm). Because sulforhodamine B dye remained in the external solution during T tubular imaging, the high fluorescence outside the fiber was eliminated after using the background subtraction rolling ball algorithm process in ImageJ (ImageJ, NIH, Bethesda, MD; http://rsb.info.nih.gov/ij/); *2*) membrane marker FM4–64: FDB fibers were loaded with the lypophilic styryl membrane marker FM4–64 (4 μM; Invitrogen) in Ringer solution for 5 min. High-resolution images (excitation: 488 nm; emission: >650 nm) were obtained on a Zeiss

LSM 510 with a ×63 NA 1.4 oil objective. Pixel dimensions were 0.12 × 0.12 μm in *x* and *y* and 0.2 μm in the *z*-axis. Deconvolution and three-dimensional reconstruction was performed using the commercially available software package Volocity (Improvision); *3*) di-8-ANEPPS staining: FDB fibers were stained with the voltage-sensitive dye pyridinium, 4-[2-(6-(dioctylamino)-2-naphthalenyl) ethenyl]-1-(3-sulfopropyl)-, inner salt (di-8-ANEPPS) (5 μM; in Ringer solution for 1 h; excitation: 488 nm; emission: >600 nm; Invitrogen). Fibers stained with di-8-ANEPPS were imaged on a Bio-Rad CellMap IC LSMC system (×60, 1.3 NA water-immersion objective; pixel dimensions 0.15 × 0.15 μm in *x* and *y*). Alternatively, di-8-ANEPPS-stained fibers were imaged on a Fluoview 500 LSCM system (×60, 1.3 NA water-immersion objective; pixel dimensions 0.2 × 0.2 μm in *x* and *y*). Images of the T tubular network were obtained with 512 × 512 pixel *x-y* images (average of 16 images). Some di-8-ANEPPS-stained fibers were also loaded with fluo 4 (20 μM; 1 h) to monitor Ca^{2+} sparks. For sequential imaging of Ca^{2+} sparks and T tubule networks, fluo 4 and di-8-ANEPPS were excited at 488 nm, and emission intensity was measured using BP 520/40-nm and a LP 600-nm filters, respectively.

RESULTS

Effects of serum treatment on muscle fiber morphology

As previously observed (2), adult FDB myofibers cultured in serum-containing media retained their morphology until approximately *day 5*, at which time the myofibers begin to dedifferentiate (Fig. 1). Dedifferentiation was characterized by sprouting at the myofiber ends and in some cases in the middle of the myofiber. In addition to sprouting, the normal striated appearance characteristic of freshly dissociated fibers became intermittent and irregular in myofibers cultured for ≥5 days. Furthermore, free cells, presumably fibroblasts from the connective tissue and freed satellite cells, proliferated and reached confluency by *day 5*. In many cases, it was apparent that these proliferating cells fused with each other and possibly with the muscle fibers. However, dedifferentiating myofibers could readily be distinguished from newly formed myotubes (Fig. 1) until approximately *day 10* in culture. At this time, both fibers and myotubes appeared as flattened, fused structures (not shown).

Time course of appearance of Ca^{2+} release events in cultured muscle fibers

In our previous study, multiple or delayed Ca^{2+} transients in response to a single field stimulus were observed in dedifferentiated fibers cultured in serum-containing media but were not observed in any fibers cultured in serum-free media. Based on these findings, as well as the gross morphology under the light microscope, we hypothesized that alterations in T tubular structure and a concomitant disorganization of EC coupling proteins may account for these observations. Our first aim in the present study was to monitor the occurrence of Ca^{2+} sparks using fluo 4 fluorescence images from fibers cultured in serum-containing media. We reasoned that if the normal EC coupling architecture was altered (locally disrupted DHPR-RyR interactions) spontaneous localized Ca^{2+} release events may be revealed. Ca^{2+} release events, indicated by local elevations of fluo 4 fluorescence, were exceedingly rare in adult mouse skeletal muscle fibers during the first days in culture (Fig. 2*A*). In contrast, Ca^{2+} events became increasingly evident in adult mouse skeletal muscle fibers between 5 and 7 days in culture in serum-containing medium (Fig. 2*B*). As described above, this time of myofiber culture often resulted in significant myofiber sprouting, a condition that was evident in Fig. 2*B*, *left*.

Figure 3*A* presents 50 successive raw *x-y* fluo 4 fluorescence images recorded at the myofiber end in a fiber from a 7-day culture. In Fig. 3*B*, the same image sequence is displayed as a ΔF series in which the ROIs of identified sparks (>2 SD above mean fiber F) are displayed. In the images collected, we observed the events to be of variable spatial extent, and there were numerous instances of Ca^{2+} events recurring at the same location in successive image frames

(Fig. 3*B*). For example, *frames 20–22* each had a detected event at the same location near the center, toward the end of the fiber, whereas *frames 24–29* each showed an event at the same location at another spot in the fiber (Fig. 3*B*). Because each *x-y* image is a "snap shot" acquired over a particular brief interval of time, we cannot tell from *x-y* images whether the events were continuous between frames or were turning off and back on between *x-y* image frames.

With the use of line scan imaging, both rapidly rising and decaying fluorescence signals (Fig. 4, *A*, *B*, and *F*), similar to Ca^{2+} sparks in frog and mammalian myofibers, and much slower rising and decaying events (Fig. 4, *C*, *D*, and *E*), as seen in developing mammalian myofibers, were observed. Taken together, either long-duration events or repetitively occurring events (both seen in Fig. 4) could account for the appearance of events that occur in the same spatial location in successive *x-y* frames (Fig. 3*B*).

Appearance of Ca^{2+} events between 5 and 7 days in culture coincides with changes in morphology indicative of dedifferentiation

Fibers dedifferentiating in serum-containing medium did not begin to exhibit Ca^{2+} events until after 3 days in culture (Fig. 5*A*). Fibers from the same culture that maintained their normal morphology did not begin to show Ca^{2+} events until after 5 days in culture. After 5 days in culture, the average rate of occurrence of Ca^{2+} sparks was more than 20-fold higher in the dedifferentiating fibers than in the fibers that appeared normal after 5 days in culture. Unlike the serum-containing cultures, fibers maintained in serum-free media exhibited very few Ca^{2+} events during a culture period of up to 7 days (Fig. 5*A*), even though dedifferentiation was seen in some fibers. Thus some serum factor may be needed in addition to dedifferentiation for the occurrence of Ca^{2+} release events. We have previously shown that, similar to FDB muscle fibers cultured in serum-free media, resting $[Ca^{2+}]$ values were not statistically different in FDB muscle fibers cultured in serum-containing media during the time of culture from *day 1* to *day 4* (2). Here we also used the ratiometric methods with indo 1-loaded FDB fibers for evaluating resting $[Ca^{2+}]$ during the time of culture at *days 1* and *3* (differentiated stage) and *days 5* and *7* (dedifferentiated stage) in FDB fibers cultured in serum-containing media. Figure 5*B* shows that resting $[Ca^{2+}]$ in FDB fibers cultured in serum-containing media is maintained around 60 nM during the time of culture from *day 1* to *day 7*. Average resting $[Ca^{2+}]$ values from *days 3, 5*, and *7* were not statistically different from *day 1* at $P < 0.05$. Thus the increase in event frequency during fiber dedifferentiation over time in serum-containing media cannot be attributed to a rise in resting $[Ca^{2+}]$ since indo 1 fluorescence ratio measurements indicted no significant change in $[Ca^{2+}]$ from 1 to 7 days in culture (Fig. 5*B*).

Ca^{2+} release events are suppressed in the presence of specific and nonspecific blockers of DHPR Ca^{2+} entry

Ca^{2+} sparks are easily detected in embryonic skeletal muscle but disappear with development and are suppressed by DHPR Ca^{2+} channel blockers (6). We hypothesized that the time points at which Ca^{2+} sparks were seen in the dedifferentiation process (i.e., increasing with T tubule disorganization) were a mirror image to the embryonic development process in which Ca^{2+} sparks disappear with T tubule maturation (6,23). Because Ca^{2+} spark activation during development was modulated by extracellular Ca^{2+} influx, we next evaluated the effect of blockers of Ca^{2+} entry on the occurrence of Ca^{2+} release events in cultured FDB fibers. We first examined the effect of $CoCl_2$, a nonspecific Ca^{2+} channel blocker. Dedifferentiated fibers cultured for 6–7 days were bathed in a Ringer solution and then imaged both before and after the addition of 5 mM $CoCl_2$. Spark frequency was almost completely suppressed 15 min after application of $CoCl_2$ (Fig. 6*A*), indicating extracellular Ca^{2+} influx may play a role in spark occurrence. Because the primary Ca^{2+} current in adult mammalian skeletal muscle is contributed by L-type Ca^{2+} channels, we then monitored the Ca^{2+} event rate after blocking L-type channels with nifedipine. Spark frequency significantly decreased in the first images taken

a few minutes after solution change and was completely suppressed after 5 min exposure to nifedepine (5 μM; Fig. 6*C*). Our results with $CoCl_2$ and nifedipine indicate that Ca^{2+} influx through the L-type Ca^{2+} channels modulates the rate of Ca^{2+} release events in dedifferentiating fibers.

In the presence of either $CoCl_2$ or nifedipine, resting fiber fluorescence increased during the time course of Ca^{2+} event measurements (Fig. 6, *B* and *D*). This finding could potentially indicate a loss in SR Ca^{2+} to the cytosol, which might have resulted in partial SR depletion and thus a decrease in spark frequency. This is unlikely, however, since control experiments without the Ca^{2+} channel antagonists (Fig. 6, *E* and *F*) demonstrate that basal fiber fluorescence rose with a similar magnitude either with or without nifedipine or $CoCl_2$. A tractable hypothesis to explain the rise in fluorescence level is nonevent Ca^{2+} release (21, 22) occurring in the fibers, an effect independent of use of the Ca^{2+} channel blockers.

Azumolene, a Ca^{2+} release modulator that suppresses the activity of the SR RyR Ca^{2+} release channel (28), was used to address its effect on the activity of Ca^{2+} sparks on *day 7* dedifferentiated fibers. In fluo 4-loaded *day 7* dedifferentiated fibers azumolene treatment (10 μM for 10 min) completely suppressed Ca^{2+} release events, indicating that RyR channel activity underlies increased Ca^{2+} sparks (data not shown). However, according to Zhao et al. (29) the effects of azumolene at the level of Ca^{2+} influx cannot be excluded. Thus further work is required *1*) to determine if store-operated Ca^{2+} entry is present in dedifferentiated fibers cultured for seven or more days and *2*) to evaluate the effect of azumolene on Ca^{2+} influx and Ca^{2+} sparks.

Appearance of Ca^{2+} release events coincides with changes in T tubule morphology

Based on the increased rate of Ca^{2+} spark occurrence coinciding with gross morphological changes seen at the light microscopic level, we next sought to evaluate T tubule morphology during the time points at which Ca^{2+} sparks were evident. We first used the extracellular marker dye sulforhodamine B. Muscle fibers cultured for only 1 day exhibited a normal striated pattern in scattered light (nonconfocal images; Fig. 7*A*) and, during exposure to sulforhodamine B (Fig. 7*A*′), showed a regular striated pattern running transversely across the fiber, suggesting a normal intact T tubule system. By *day 7*, cultured muscle fibers showed varying degrees of T tubule disorganization as indicated by the intermittent disruption of the transverse pattern of sulforhodamine B staining and the appearance of a longitudinal network of the T tubule system (Fig. 7, *B*′ and *C*′). Even those fibers that appeared to have a normal striated appearance in scattered light images (Fig. 7*B*) showed some degree of T tubule disruption, as indicated by the breakdown of the transverse network and the appearance of the longitudinal network of the T tubule system (Fig. 7*B*′). These fibers may be in the early stages of dedifferentiation. Those fibers that were fully dedifferentiated did not have the transverse sarcomeric pattern in scattered light images (Fig. 7*C*′) and exhibited more pronounced changes in the T tubule morphology, as indicated by the presence of a larger number of longitudinal bands within the T tubule system.

T tubule morphology was further examined using the dyes di-8-ANEPPS or FM4–64, both of which stain membranes exposed to extracellular solution. In adult mammalian skeletal muscle, the T tubule system displays a highly organized transverse pattern. In Fig. 8, T tubules were visualized by staining the fibers with 5 μM di-8-ANEPPS. In *day 1* differentiated fibers (Fig. 8, *B* and *C*), T tubules were organized in a regular striated pattern, characterized by a ~2-μm sarcomere length and ~1 μm spacing between T tubule doublets. In *day 7* dedifferentiated fibers (Fig. 8, *E* and *F*), the T tubular structure was reorganized and characterized by an apparent reduction in the T tubule doublet spacing, whereas more pronounced reorganization was observed near to and at the center of the sprouting site, where an almost complete disruption of the T tubules was observed (Figs. 9*C* and 10*C*). Figure 9 shows images of the T tubule system stained with FM4–64 in adult FDB fibers cultured for either 1 (Fig. 9*A*) or 7 (Fig. 9,

B and *C*) days. After 1 day of culture, FDB myofibers retain the transverse spatial pattern indicative of adult skeletal muscle. After 7 days in culture, T tubule alterations were observed, with appearance of longitudinal T tubules (Fig. 9*B*) and as a chaotic reorganization of the T tubules (Fig. 9*C*).

Recent data by Zhou et al. (31) suggest that the DHPR, which resides in the T tubule membrane, suppresses Ca^{2+} sparks. Thus the appearance of Ca^{2+} sparks in our experiments might be because of this profound reorganization of the T tubules. We directly examined the relationship between changes in T tubule organization and Ca^{2+} spark activity by staining fluo-4-loaded *day 7* dedifferentiated fibers with di-8-ANEPPS and imaged two sequential emission bands. Despite the emission cross talk between the fluo 4 and di-8-ANEPPS signal, the dynamic range of the fluo 4 and the constant di-8-ANEPPS intensity allowed for monitoring of the occurrence of sparks. Figure 10*B* shows a representative image of a series of images of fluo 4 fluorescence (50 frames), illustrating the locations where sparks were more frequent. Figure 10*C* shows the fluorescence (average of 8 frames) of di-8-ANEPPS in the same region. Note that, in regions where sparks were frequent, T tubule structures were not present or appeared disorganized.

DISCUSSION

Ca^{2+} sparks are discrete, localized, microscopic elevations of Ca^{2+} that are the result of the synchronized opening and closing of a small number of RyR Ca^{2+} release channels (4,24,13). Under normal conditions, Ca^{2+} sparks are thought to underlie the macroscopic efflux of Ca^{2+} from the RyR Ca^{2+} channels in the SR that occurs following depolarization of a frog skeletal muscle fiber (14,15,30). Thus Ca^{2+} sparks represent fundamental events in frog skeletal muscle EC coupling. In contrast, previous studies have shown that Ca^{2+} sparks are rarely seen in intact adult mammalian skeletal muscle (19,22). Our new studies presented here identify and quantitate the reappearance and increasing frequency of Ca^{2+} sparks during various stages of dedifferentiation in adult mouse skeletal muscle fibers maintained in culture.

Dedifferentiation of adult FDB fibers in culture is characterized by pronounced changes in muscle fiber morphology. These changes, including loss of striations and the appearance of cytoplasmic sprouts coming out of the ends or sides of dedifferentiating fibers, can occur along the length of the fiber. The exact mechanisms underlying the observed dedifferentiation to a myotube-like structure are not known, but the morphological changes are more pronounced and enhanced by the presence of serum in the culture media (2). During this period of pronounced changes, at approximately five to seven days in serum-containing media, Ca^{2+} spark activity increased 25-fold when compared with fibers only cultured for one day in serum-containing media. However, results from fibers cultured in serum-free media indicate that, although dedifferentiation may be necessary for the appearance of Ca^{2+} release events, it may not be sufficient, and some serum factor may also be needed.

The morphological changes observed using transmitted light microscopy were also accompanied by morphological changes in the T tubular system, as observed using sulforhodamine B as an extracellular marker for the T tubule lumen or using di-8-ANEPPS or FM4–64 membrane staining and confocal fluorescence imaging. There appeared to be a transition from a transverse to a longitudinal pattern of T tubule staining as the fibers progressed toward the morphologically dedifferentiated state. A similar longitudinal orientation has previously been described and is characteristic of the early phase of T tubule development (11,23). The orderly, transverse orientation of the T tubule occurs late in development. Thus, when dedifferentiation occurs, the transition in the T tubule orientation may indicate a transition from the mature, fully developed muscle fiber back toward an earlier developmental stage of the muscle fiber. This further supports our hypothesis that dedifferentiation may be the reverse of the development of myotubes to mature muscle fibers. There is currently considerable

interest in the mechanisms underlying cellular dedifferentiation (17,25) and the possibility of using dedifferentiated cells for tissue repairs and/or in the production of various forms of engineered tissues. It will be interesting to determine whether the local Ca^{2+} release events detected here in morphologically dedifferentiating skeletal muscle fibers may play a signaling or functional role in the muscle fiber dedifferentiation process.

A direct correlation between spatial distribution of the Ca^{2+} sparks and the areas of T tubule disruption was made, and it is clear that, as the disruption of the T tubule system progressed over time in culture, there was also an increase in the number of Ca^{2+} events. Thus the appearance of the Ca^{2+} sparks when the fibers begin to dedifferentiate may point to Ca^{2+} sparks being a signal for, or the result of, disruption of DHPR-RyR1 coupling. Recently, Zhou et al. (31) showed similar results when examining Ca^{2+} sparks in primary cultures of mammalian myotubes. In their studies, Ca^{2+} sparks were not detected along the periphery of the myotube, which is the primary region in which the T tubule system was developed. In contrast, Ca^{2+} events were detected in the central regions of the myotubes, i.e., in T tubule-free regions. In our studies, Ca^{2+} sparks were detected along the periphery and in the center of the dedifferentiating fibers. Likewise, T tubule disorganization was observed in the periphery and in the central regions of the fibers. We also observed that the sparks that appear in the dedifferentiating muscle fibers were suppressed in the presence of either the specific DHPR channel blocker nifedipine or the nonspecific Ca^{2+} channel blocker Co^{2+}. These observations suggest that Ca^{2+} sparks may be generated by similar mechanisms in dedifferentiating cultured adult fibers as in embryonic fibers in which Ca^{2+} sparks are also blocked by the same specific and nonspecific DHPR channel blockers (6).

In conclusion, Ca^{2+} sparks appear in dedifferentiating adult skeletal muscle fibers. Our observations with T tubule staining, with Ca^{2+} channel blockers, and of the spatial distribution of Ca^{2+} sparks suggest that dedifferentiation may be a transition toward the embryonic state of muscle development and that Ca^{2+} spark occurrence is coincident with disruption of the normal T tubule and SR structure seen in normal, healthy adult skeletal muscle fibers. In this regard, the appearance of Ca^{2+} sparks in adult muscle may provide an indication of localized T tubule disruption.

References

1. Block BA, Imagawa T, Campbell KP, Franzini-Armstrong C. Structural evidence for direct interaction between the molecular components of the transverse tubule-sarcoplasmic reticulum junction in skeletal muscle. J Cell Biol 1988;107:2587–2600. [PubMed: 2849609]
2. Brown LD, Schneider MF. Delayed differentiation and retention of properties in dissociated adult skeletal muscle fibers in vitro. In Vitro Cell Dev Biol-Animal 2002;38:411–422.
3. Chen YW, Zhao P, Borup R, Hoffmann EP. Expression profiling in the muscular dystrophies: identification of novel aspects of molecular patho-physiology. J Cell Biol 2000;151:1321–1336. [PubMed: 11121445]
4. Cheng H, Lederer WJ, Cannell MB. Calcium sparks: elementary events underlying excitation-contraction coupling in heart muscle. Science 1993;262:740–744. [PubMed: 8235594]
5. Cheng H, Song LS, Shirokova N, Gonzalez A, Lakatta EG, Rios E, Stern MD. Amplitude distribution of calcium sparks in confocal images: theory and studies with an automatic detection method. Biophys J 1999;76:606–617. [PubMed: 9929467]
6. Chun LG, Ward CW, Schneider MF. Ca^{2+} sparks are initiated by Ca^{2+} entry in embryonic mouse skeletal muscle and decrease in frequency postnatally. Am J Physiol Cell Physiol 2003;285:C686–C697. [PubMed: 12724135]
7. Conklin MW, Barone V, Sorrentino V, Coronado R. Contribution of ryanodine receptor type 3 to Ca^{2+} sparks in embryonic mouse skeletal muscle. Biophys J 1999;77:1394–1403. [PubMed: 10465751]

8. Duckmanton A, Kumar A, Chang YT, Brockes JP. A single-cell analysis of myogenic dedifferentiation induced by small molecules. Chem Biol 2005;12:1117–1126. [PubMed: 16242654]
9. Endo M. Entry of a dye into the sarcotubular system of muscle. Nature 1964;202:1115–1116. [PubMed: 14207209]
10. Felder E, Franzini-Armstrong C. Type 3 ryanodine receptors of skeletal muscle are segregated in a parajunctional position. Proc Natl Acad Sci USA 2002;99:1695–1700. [PubMed: 11818557]
11. Franzini-Armstrong C. Simultaneous maturation of transverse tubules and sarcoplasmic reticulum during muscle differentiation in the mouse. Dev Biol 1991;146:353–363. [PubMed: 1864461]
12. Grynkiewicz G, Poenie M, Tsien RY. A new generation of Ca^{2+} indicators with greatly improved fluorescence properties. J Biol Chem 1985;260:3440–3450. [PubMed: 3838314]
13. Kirsch WG, Uttenweiler D, Fink RH. Spark- and ember-like elementary Ca^{2+} release events in skinned fibers of adult mammalian skeletal muscle. J Physiol 2001;537:379–89. [PubMed: 11731572]
14. Klein MG, Cheng H, Santana LF, Lederer WJ, Schneider MF. Two mechanisms of quantized calcium release in skeletal muscle. Nature 1996;379:455–458. [PubMed: 8559251]
15. Klein MG, Schneider MF. Ca^{2+} sparks in skeletal muscle. Prog Biophys Mol Biol 2006;92:308–332. [PubMed: 16125755]
16. Liu Y, Carroll SL, Klein MG, Schneider MF. Calcium transients and calcium homeostasis in adult mouse fast-twitch skeletal muscle fibers in culture. Am J Physiol Cell Physiol 1997;272:C1919–C1927.
17. Palacios D, Puri PL. The epigenetic network regulating muscle development and regeneration. J Cell Physiol 2006;207:1–11. [PubMed: 16155926]
18. Perez OD, Chang YT, Rosania G, Sutherlin D, Schultz PG. Inhibition and reversal of myogenic dedifferentiation by purine-based microtubule assembly inhibitors. Chem Biol 2002;9:474–483.
19. Rios E. The Ca^{2+} spark of mammalian muscle. Physiology or pathology? (Abstract). J Physiol 2005;565:705. [PubMed: 15878940]
20. Rodney GG, Schneider MF. Calmodulin modulates initiation but not termination of spontaneous Ca^{2+} sparks in frog skeletal muscle. Biophys J 2003;85:921–932. [PubMed: 12885639]
21. Shirokova N, Rios E. Small event Ca^{2+} release: a probable precursor of Ca^{2+} sparks in frog skeletal muscle. J Physiol 1997;502:3–11. [PubMed: 9234193]
22. Shirokova N, Garcia J, Rios E. Local calcium release in mammalian skeletal muscle. J Physiol 1998;512:377–384. [PubMed: 9763628]
23. Takekura H, Flucher BE, Franzini-Armstrong C. Sequential docking, molecular differentiation, and positioning of T-tubule/SR junctions in developing mouse skeletal muscle. Dev Biol 2001;239:204–214. [PubMed: 11784029]
24. Tsugorka A, Rios E, Blatter LA. Imaging elementary events of calcium release in skeletal muscle cells. Science 1995;269:1723–1726. [PubMed: 7569901]
25. Wagers AJ, Conboy IM. Cellular and molecular signatures of muscle regeneration: current concepts and controversies in adult myogenesis. Cell 2005;122:659–667. [PubMed: 16143100]
26. Wang X, Weisleder N, Collet C, Zhou J, Chu Y, Hirata Y, Zhao X, Pan Z, Brotto M, Cheng H, Ma J. Uncontrolled calcium sparks act as a dystrophic signal for mammalian skeletal muscle. Nat Cell Biol 2005;7:525–530. [PubMed: 15834406]
27. Ward CW, Protasi F, Castillo D, Wang Y, Chen SR, Pessah IN, Allen PD, Schneider MF. Type 1 and type 3 ryanodine receptors generate different $Ca(^{2+})$ release event activity in both intact and permeabilized myotubes. Biophys J 2001;81:3216–3230. [PubMed: 11720987]
28. Zhang Y, Rodney GG, Schneider MF. Effects of azumolene on Ca^{2+} sparks in skeletal muscle fibers. J Pharmacol Exp Ther 2005;314:94–102. [PubMed: 15831441]
29. Zhao X, Weisleder N, Han X, Pan Z, Parness J, Brotto M, Ma J. Azumolene inhibits a component of store-operated calcium entry coupled to the skeletal muscle ryanodine receptor. J Biol Chem 2006;281:33477–33486. [PubMed: 16945924]
30. Zhou J, Launikonis BS, Rios E, Brum G. Regulation of Ca^{2+} sparks by Ca^{2+} and Mg^{2+} in mammalian and amphibian muscle. An RyR isoform-specific role in excitation-contraction coupling? J Gen Physiol 2004;124:409–428. [PubMed: 15452201]

31. Zhou J, Yi J, Royer L, Launikonis BS, Gonzalez A, Garcia J, Rios E. A probable role of dihydropyridine receptors of Ca^{2+} sparks, demonstrated in cultured mammalian muscle. Am J Physiol Cell Physiol 2006;290:C539–C553. [PubMed: 16148029]

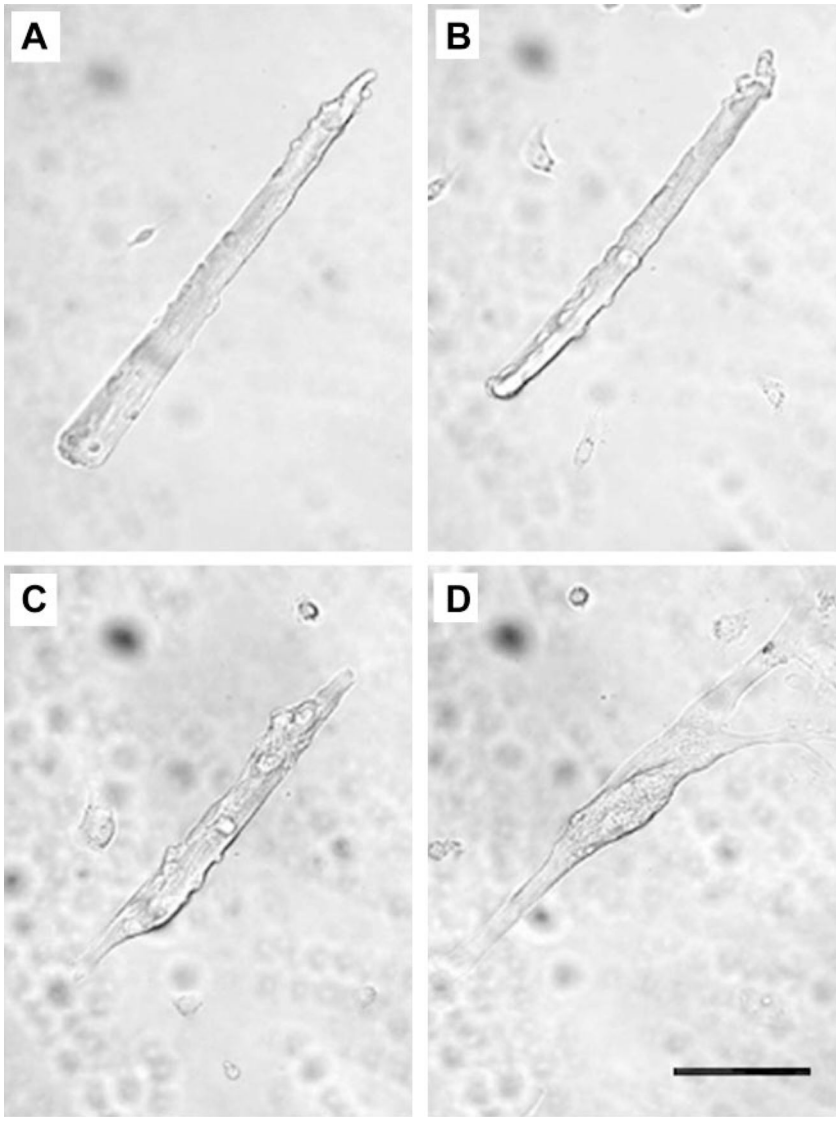

Fig. 1.

A single representative isolated adult flexor digitorum brevis (FDB) muscle fiber cultured on a laminin-coated cover slip in serum-containing media. Transmitted light images of the same fiber were taken 1 day (*A*), 3 days (*B*), 5 days (*C*), and 7 days (*D*) after plating. The images show the gradual transition from the adult fiber appearance to a myotube-like morphology, including branches and fine projections. The culture was returned to the tissue culture incubator for 2-day intervals between acquisitions of successive images. Scale bar = 0.1 mm.

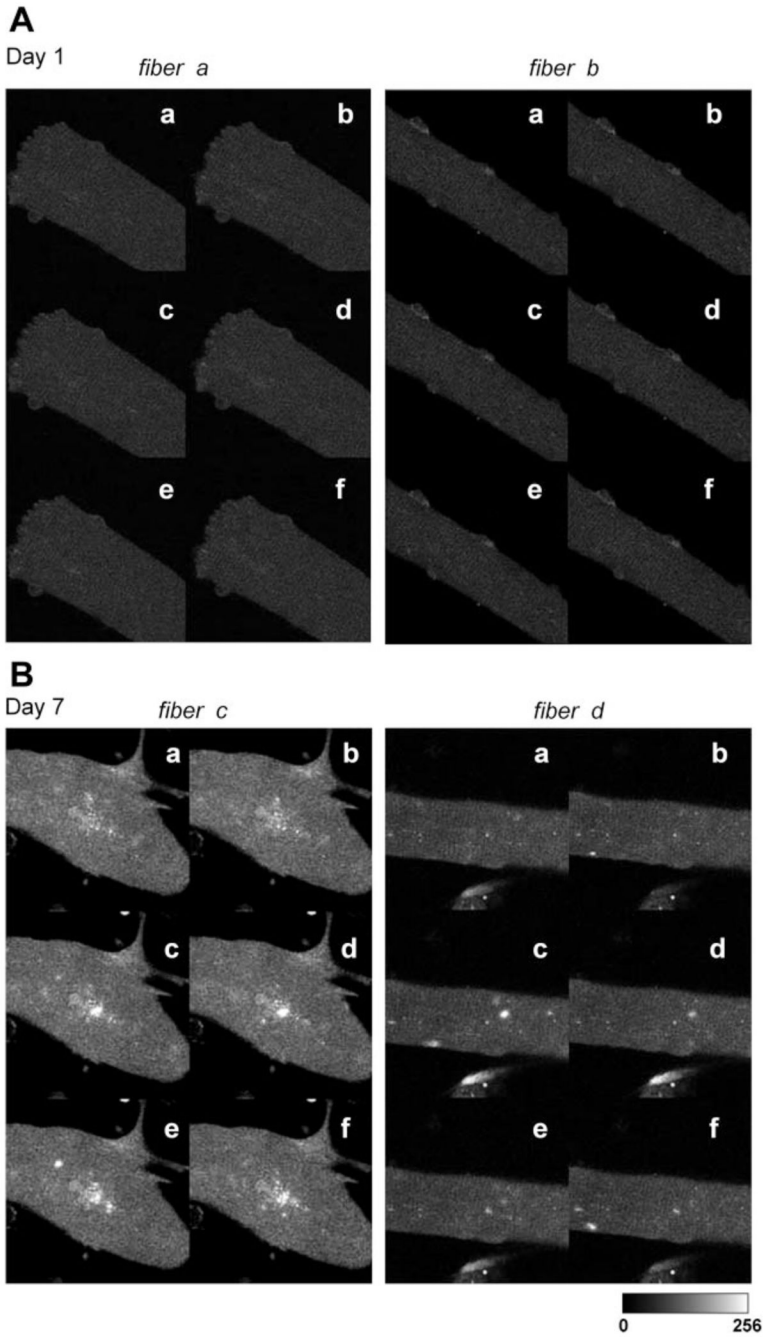

Fig. 2.

Local Ca^{2+} sparks events in single muscle fibers after 1 day (*A*) and after 7 days (*B*) in culture. Six representative images of 2 different fibers are shown for each condition (*a–f*). Note the appearance of Ca^{2+} events in the fibers cultured for 7 days.

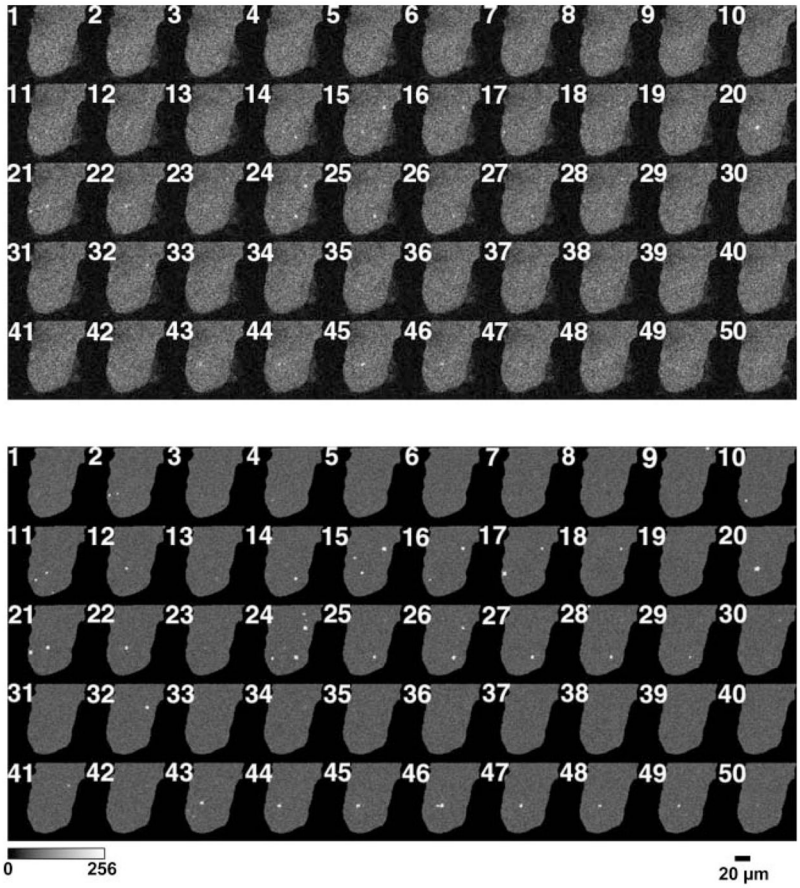

Fig. 3.

Ca^{2+} sparks appear in both the periphery and the center of dedifferentiating muscle fibers. *A*: 50 sequential full-frame fluorescence images of a muscle fiber loaded with fluo 4 after being maintained in a serum-containing culture for 7 days. *B*: events selected from *A* as being within the selection criteria of contiguous pixels >2 SD above the mean of the same pixel, with at least one pixel >3 SD above the mean. Each selected event is shown within an enclosing box in the image. Successive images were recorded at 3-s intervals.

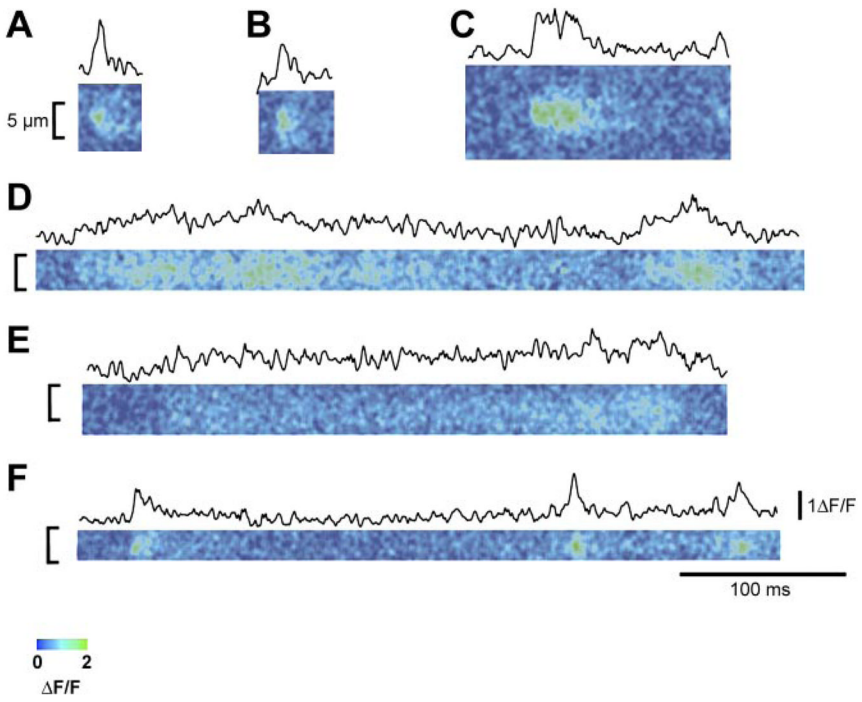

Fig. 4.

ΔF/F (where F is fluorescence) line scan images from intact dedifferentiating adult mouse muscle fibers. Above each ΔF/F image is the mean temporal profile centered at the peak ΔF/F. These records represent a sampling of the various different time courses of local Ca^{2+} release events recorded from dedifferentiating fibers using line scan imaging. *A*, *B*, and *F*: line scan images and time courses of both rapidly rising and decaying fluorescence signals. Note that these signals are quite similar to Ca^{2+} sparks observed in frog and mammalian myofibers. *C*, *D*, and *E*: line scan images and time courses of slower rising and decaying events. Note that these records are similar to Ca^{2+} signals as seen in developing mammalian myofibers.

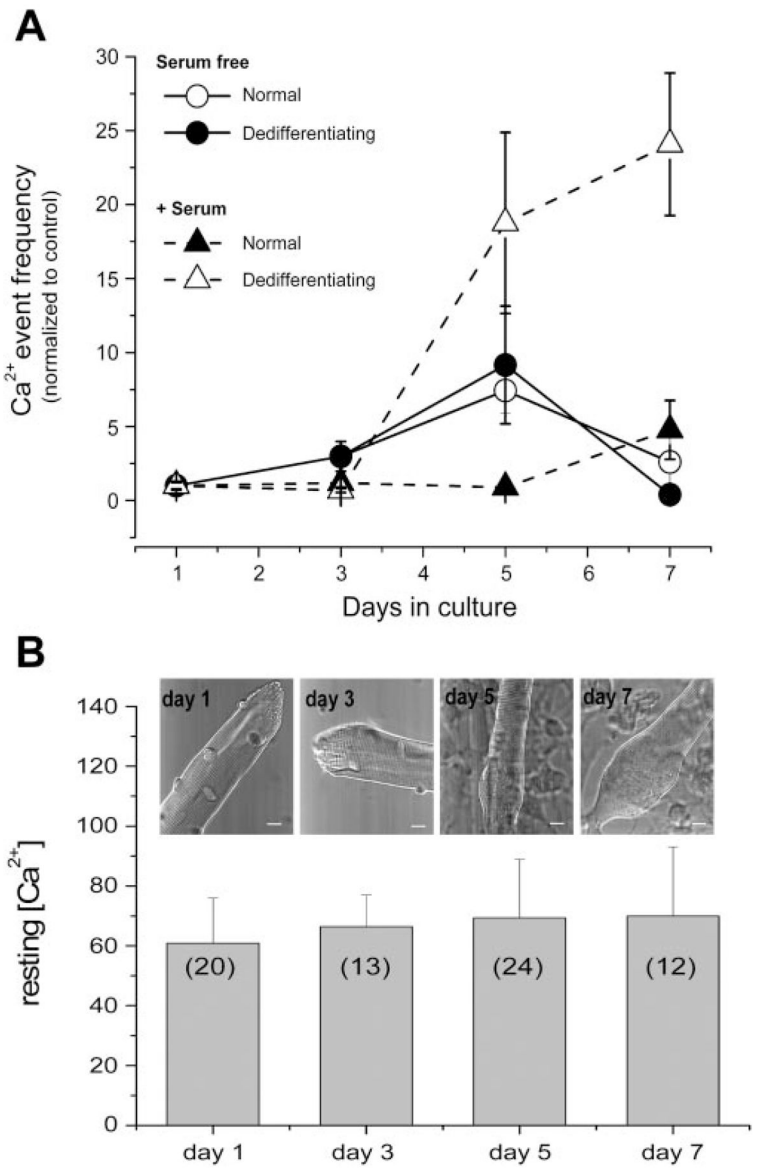

Fig. 5.

Frequency of Ca^{2+} events in both normal and dedifferentiated adult FDB fibers and resting Ca^{2+} concentration ($[Ca^{2+}]$) after various times in culture. *A*: fibers were cultured in either serum-containing media or serum-free media. Frequency of Ca^{2+} event fibers increases as fiber dedifferentiation increases. In serum-containing media, the no. of fibers included with normal appearance was 15, 20, 9, and 3 and 0, 0, 11, and 5 with dedifferentiated appearance at the successive time points, and in serum-free media was 25, 16, 19, and 10 with normal appearance and 0, 2, 5, and 7 with dedifferentiated appearance at the successive time points. Statistical significance was determined using a 2-way ANOVA test. Significance ($P < 0.05$) was found between the dedifferentiating fibers in serum-containing media and all the other groups at both *days 5* and *7*. *B*: intracellular resting $[Ca^{2+}]$ during fiber dedifferentiation. Bar graph summarizing mean resting $[Ca^{2+}]$ evaluated by ratiometric photometry in indo 1-loaded FDB fibers cultured in serum-containing media at four different stages (*days 1*, 3,5, and 7) after fiber plating. Transmitted light images at *top* of each column shows the typical appearance of FDB fibers for each stage. Scale bar = 10 μm; nos. in parentheses represent sample size.

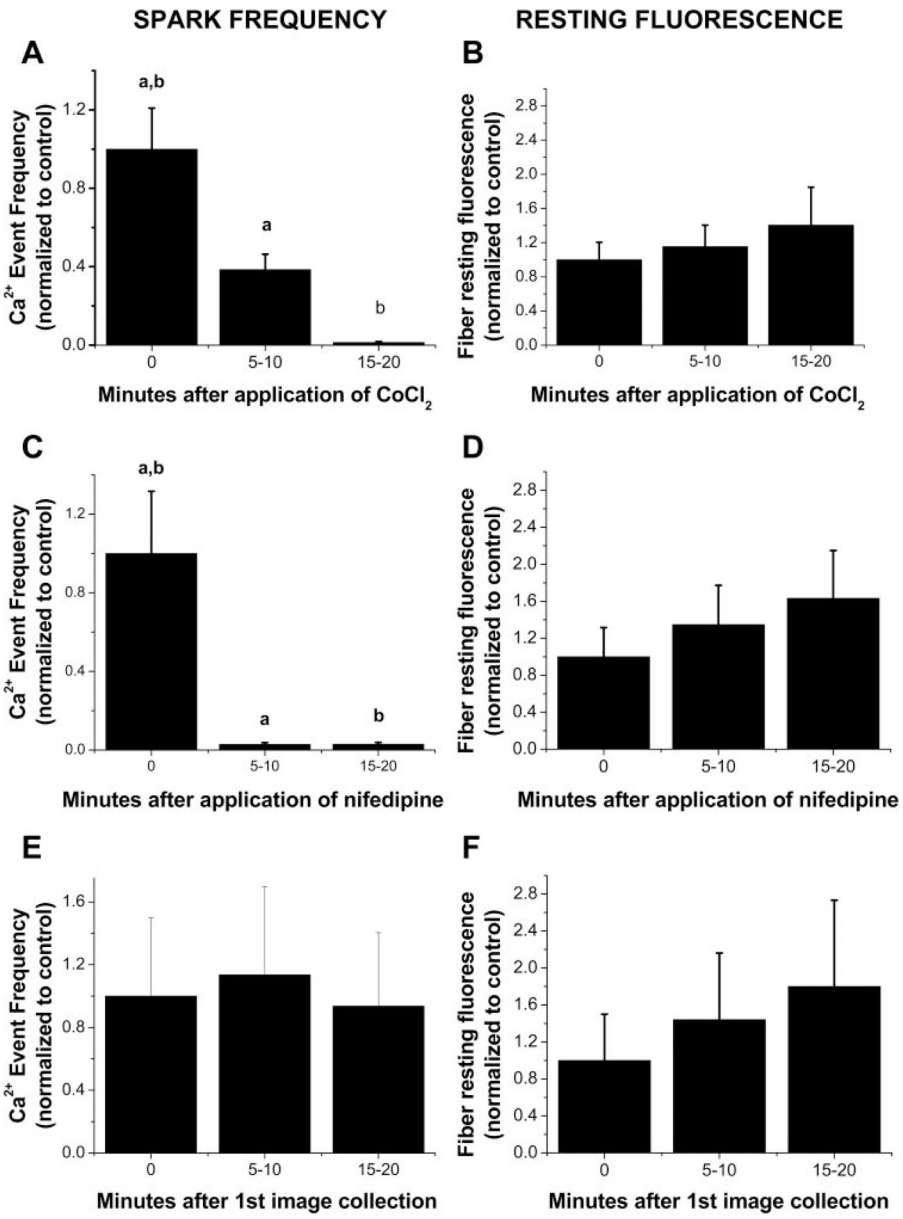

Fig. 6.

Frequency of Ca^{2+} events in dedifferentiated adult FDB fibers decreases with addition of Ca^{2+} channel blockers. All fibers were cultured for 6–7 days in $CoCl_2$-free, nifedipine-free, serum-containing medium before each experiment. *A*: fibers cultured in serum-containing media were bathed in Ringer solution and imaged both before and after the addition of 5 mM $CoCl_2$ as indicated. *B*: time course of resting fiber fluorescence in the same fibers both before and after the addition of $CoCl_2$. *C*: fibers cultured in serum-containing media were bathed in Ringer solution and imaged both before and after the addition of 5 μM nifedipine as indicated. *D*: time course of resting fiber fluorescence in the same fibers both before and after the addition of nifedipine. *E*: fibers cultured in serum-containing media were bathed in Ringer solution and imaged for spark activity without Ca^{2+} channel blocker treatment. *F*: time course of resting fiber fluorescence in the same fibers without Ca^{2+} channel blocker treatment; $n = 21$ in *A* and *B*, $n = 10$ in *C* and *D*, and $n = 10$ in *E* and *F*. Statistical significance was determined using a

1-way ANOVA test ($P < 0.05$). Groups with the same letter exhibit significant difference from each other.

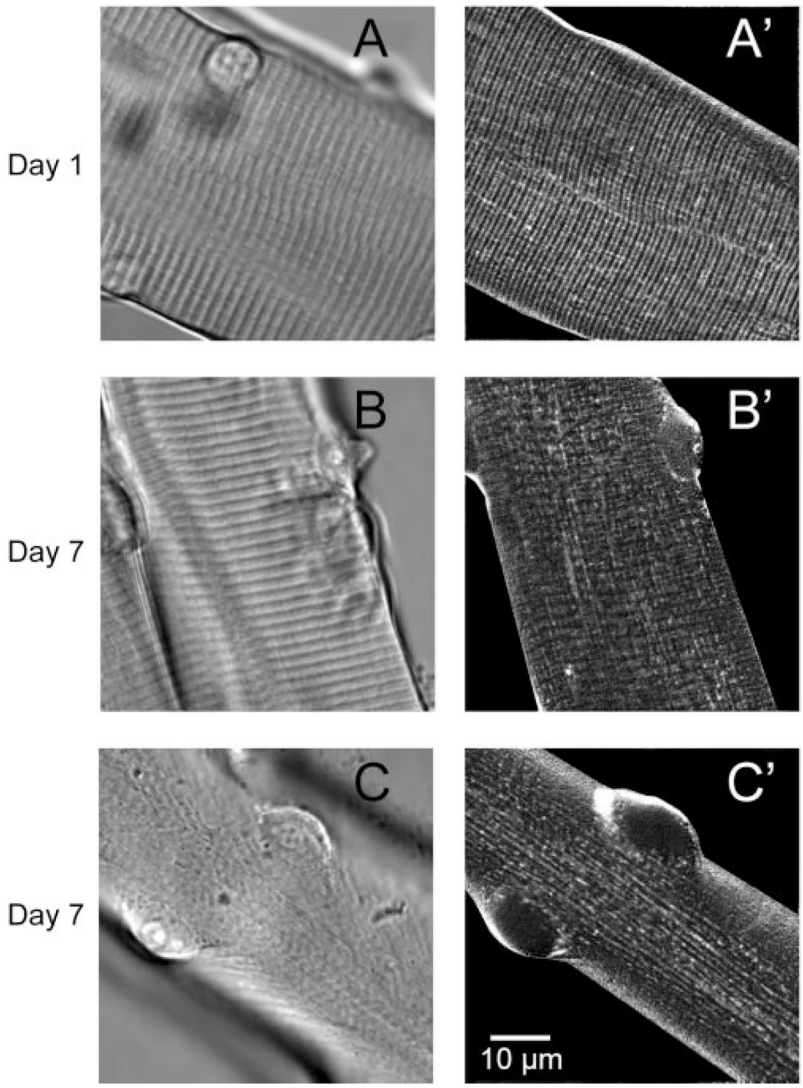

Fig. 7.

Transmitted light (*A*–*C*) and sulforhodamine B (*A*′–*C*′) images of fibers after 1 and 7 days in culture. After 1 day in culture, both transmitted light (*A*) and sulforhodamine-stained (*A*′) images showed an orderly pattern of both striations and transverse (T) tubule structure. By *day 7*, dedifferentiating fibers exhibit various stages of disruption of T tubule structure after staining with sulforhodamine B (*B*′ and *C*′). Longitudinally oriented T tubules are apparent in *C*′.

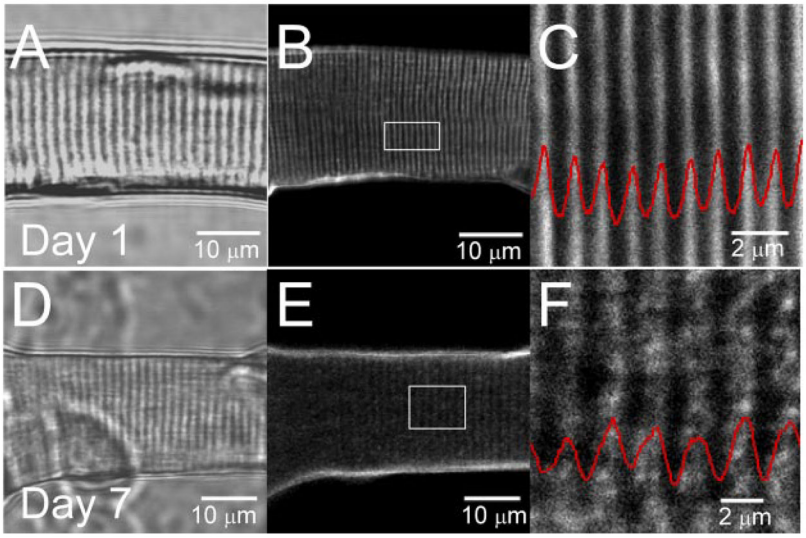

Fig. 8.

T tubule structure reorganization during fiber dedifferentiation. Transmitted light images (average of 8 frames) of FDB fibers cultured in serum-containing media after 1 (*A*) and 7 (*B*) days in culture. *B* and *E*: laser confocal images (average of 16 frames) of the same fibers stained with pyridinium, 4-[2-(6-(dioctylamino)-2-naphthalenyl) ethenyl]-1-(3-sulfopro-pyl)-, inner salt (di-8-ANEPPS) from a single *z*-axis plane. *C* and *F*: enlarged views of the outlined regions of the fibers shown in *B* and *E*, respectively. Red traces, average intensity profile, plotted as a function of the longitudinal position, of area enclosed within white rectangles in *B* and *E*. After 7 days in culture, T tubular structure was disorganized and characterized by an apparent reduction in the T tubule spacing.

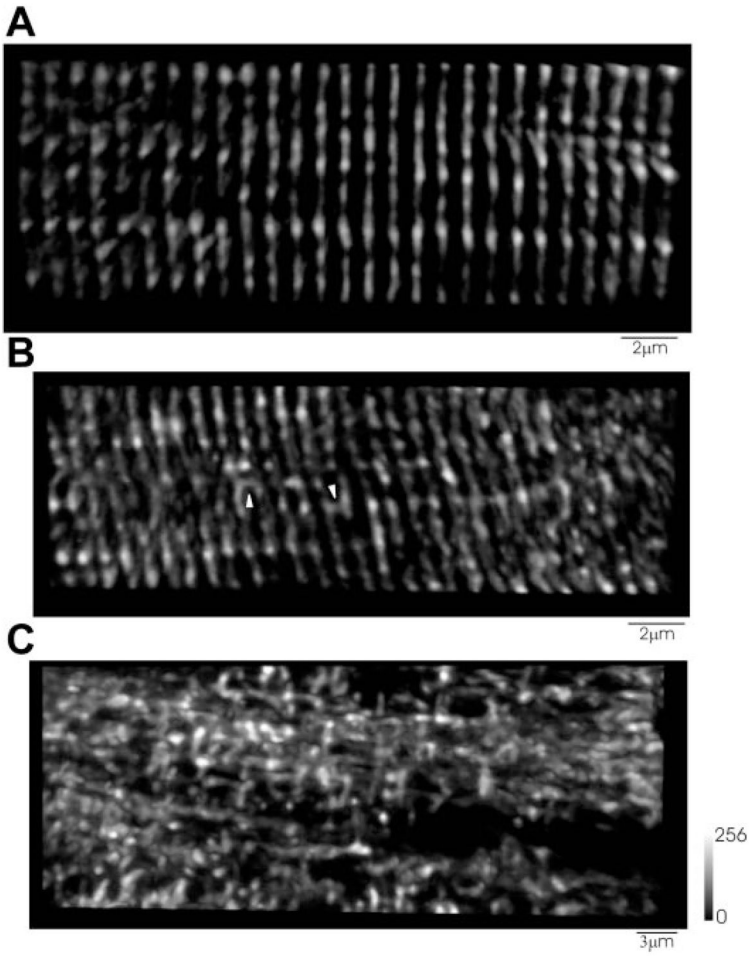

Fig. 9.

T tubule structure in fibers after culture for 1 and 7 days: FM4–64 staining. *A*: FM4–64 staining of T tubules shows a normal transverse striated pattern after 1 day in culture. *B* and *C*: after 7 days in culture, T tubules show an alteration in the transverse striated pattern, with either an occasional longitudinal T tubule (arrowhead; *B*) or (C) a complete loss of the transverse striated pattern with areas of the fiber void of T tubules (*C*).

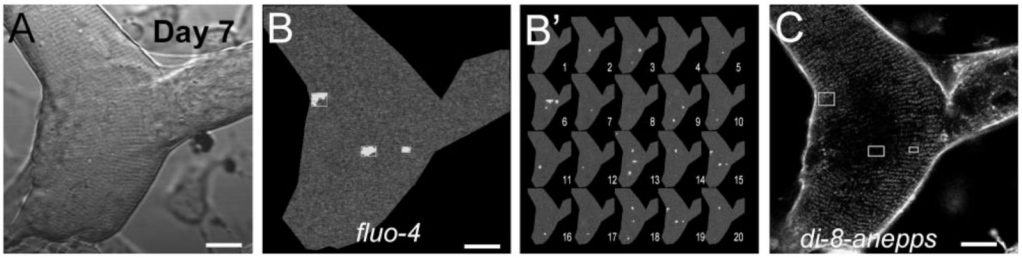

Fig. 10.

T tubule reorganization and Ca^{2+} sparks in a di-8-ANEPPS-stained and fluo 4-loaded *day 7* dedifferentiated fiber. A series of images of fluorescence of fluo-4 (50 frames) and fluorescence of di-8-ANEPPS (average of 8 images) was obtained in a sequential mode scanning in the same fiber. *A*: transmitted light image. *B*: representative single full *x-y* frame image showing Ca^{2+} sparks appearing in both the periphery and the center of *day 7* dedifferentiating muscle fiber. Each selected event is shown within an enclosing box in the image. *B′*: 20 sequential *x-y* mode images of fiber shown in *B*. Events were selected as in Fig. 3. *C*: image of fluorescence of di-8-ANEPPS, showing reorganized T tubules. For comparison, enclosing boxes showing events in *B*, were redrawn here. Note that Ca^{2+} sparks usually occur in central areas, where T tubule disruption is more dramatic. Scale bars = 10 μm.